Journal of
Materials Chemistry B

Materials for biology and medicine

Accepted Manuscript

This article can be cited before page numbers have been issued, to do this please use: X. Sun, Y. Qiao, W. Li, Y. Sui, Y. Ruan and J. Xiao, *J. Mater. Chem. B*, 2020, DOI: 10.1039/D0TB00476F.

This is an Accepted Manuscript, which has been through the Royal Society of Chemistry peer review process and has been accepted for publication.

Accepted Manuscripts are published online shortly after acceptance, before technical editing, formatting and proof reading. Using this free service, authors can make their results available to the community, in citable form, before we publish the edited article. We will replace this Accepted Manuscript with the edited and formatted Advance Article as soon as it is available.

You can find more information about Accepted Manuscripts in the Information for Authors.

Please note that technical editing may introduce minor changes to the text and/or graphics, which may alter content. The journal's standard Terms & Conditions and the Ethical guidelines still apply. In no event shall the Royal Society of Chemistry be held responsible for any errors or omissions in this Accepted Manuscript or any consequences arising from the use of any information it contains.

ROYAL SOCIETY OF CHEMISTRY

rsc.li/materials-b

ROYAL SOCIETY OF CHEMISTRY View Article Online
DOI: 10.1039/D0TB00476F

Journal of Materials Chemistry B

ARTICLE

A graphene oxide-aided triple helical aggregation-induced emission biosensor for highly specific detection of charged collagen peptides

Xiuxia Sun,[a] Yan Qiao,[a] Wenhua Li,[a] Yiyao Sui,[a] Yiyan Ruan,[a] Jianxi Xiao[a,*]

Received 00th January 20xx,
Accepted 00th January 20xx

DOI: 10.1039/x0xx00000x

www.rsc.org/

Aggregation-induced emission (AIE) probes have emerged as promising "turn-on" sensing tools for DNAs and proteins, and the AIE biosensors conjugated with graphene oxide (GO) has shown improved selectivity. Collagen is the essential structural protein in human body, and its degraded products are involved in a plethora of severe diseases. Collagen has a high content of charged amino acids, while EOG represents one of the most abundant charged triplets in Type I collagen. We herein for the first time report the construction of a GO-aided AIE biosensor for the detection of charged collagen peptides. We have shown that an AIE fluorophore TPE conjugated with a triple helical peptide TPE-PRG possesses strong fluorescence due to the restriction of intramolecular rotation of TPE in the trimer state. The adsorption of the probe TPE-PRG by GO leads to efficient fluorescence quenching, while the addition of target collagen peptide EOG releases the probe peptide from the GO surface and recovers its fluorescence. We have demonstrated that the TPE-PRG/GO complex provides a highly specific "turn-on" sensing platform for the target collagen peptide with a typical charged amino acid-rich sequence. The assay has shown little interference from other biomolecules, and it can also effectively distinguish the target charged collagen peptide from its single amino acid mutant type. The development of robust analytical assays for charged collagen peptides would pronouncedly extend our capability to investigate the pathology of collagen diseases, showing great potential in its molecular diagnostics.

Introduction

The detection of biomolecules with high sensitivity and selectivity is critical for the diagnosis and therapies for a broad variety of pathological conditions.[1-3] Due to superior sensitivity, low background noise and wide dynamic range, fluorescent biosensors have received extensive attention in the developments of bio-assays for targeting macromolecules.[4] A plethora of organic molecules based on electron transfer (ET), charge transfer (CT), and (ET) mechanisms have been created as fluorescent probes for biosensing.[5-7] However, a significant number of fluorophores suffer from drastic quenched fluorescent emissions at high concentrations due to the thorny aggregation-caused quenching (ACQ), which severely limits the scope of the practical applications of these probes with a fluorescent "turn-off" mode.[8-10] The development of fluorescent probes that can overcome the detrimental ACQ effect therefore attracts increasing interest in the field of biosensors.

A novel class of fluorophores with exactly opposite aggregation-induced emission (AIE) features have recently been discovered and widely applied in label-free and "turn-on" fluorescent biological analysis.[11-17] These AIE-active fluorophores display strong fluorescent emission when their intramolecular rotations are restricted upon binding with biomolecules or forming the aggregate state, which facilitates the AIE probes as versatile "turn-on" sensing platforms for DNAs and proteins.[18-20] It has been shown that AIE fluorophores with positive charges could strongly bind with single stranded DNA, resulting in the formation of aggregation complex of AIE probes and DNA, which gives rise to striking fluorescent enhancement of the AIE probes.[21-23] However, the AIE probes also interact with other interferential biomolecules such as RNAs and proteins, leading to insufficient selectivity of the assay.[24] It is therefore in urgent need for the construction of AIE biosensors with improved specificity.

The conjugation of AIE probes with graphene oxide (GO) has led to the creation of novel AIE-based biosensors with effectively enhanced selectivity.[25] The complex of $A_2HPS{\cdot}HCl$ (a derivative of hexaphenylsilone) and GO has been utilized to detect DNA with a detection limit of μg/mL, while the mixture of TPE-SO_3Na and GO has been applied for the highly selective detection of bovine serum albumin (BSA).[25, 26] The platforms using AIE probes supplemented with GO and single-stranded DNA (ssDNA) have been recently shown to provide rapid "turn-on" fluorescent methods for the detection of DNA with complementary sequence.[27, 28] A fluorescent aptasensor based on an AIE fluorophore DSAI, GO and ssDNA aptamers has been established for selective and sensitive sensing of targeted DNA and thrombin protein.[29] These studies have shown that the GO-aided AIE biosensors could provide a promising sensing platform for the selective detection of biomolecules.

Collagen is the most abundant protein in human body, and the degraded products of collagen are involved in a variety of diseases such as tumors, arthritis, and chronic wounds.[30-33] Extensive efforts have been dedicated to the discovery of efficient assays for collagen

[a] State Key Laboratory of Applied Organic Chemistry, Key Laboratory of Nonferrous Metal Chemistry and Resources Utilization of Gansu Province, College of Chemistry and Chemical Engineering, Lanzhou University, Lanzhou 730000, P. R. China.
[*] Corresponding author. Email address: xiaojx@lzu.edu.cn (J. Xiao).

fragments.[34-37] Due to the repetitive amino acid sequences and uniform triple helical structure, it remains challenging to create antibodies with high specificity toward collagen.[38, 39] A monoclonal IgG1 antibody has been generated to detect denatured collagen, while a tumor-homing peptide has been found to recognize the fragments of Type IV Collagen.[35, 36] However, these approaches often suffered from drawbacks such as tedious procedures and low binding affinity. We have recently discovered that FITC (fluorescein isothiocyanate)-labeled triple helical peptide $C(POG)_9$ (O, Hydroxyproline) could recognize single stranded GPO-rich peptide with the aid of graphene oxide.[40] GPO represents the most abundant triplet with neutral amino acids in collagen, while it is worth noting that collagen has a high content of charged amino acids, and Glu-Hyp-Gly is the most frequent charged amino acid triplet in Type I collagen.

We herein for the first time report the construction of a GO-supplemented AIE biosensor for the selective detection of charged collagen peptides. We have shown that an AIE fluorophore TPE conjugated with a triple helical peptide possesses strong fluorescence, which could be efficiently quenched by GO. We have demonstrated that the triple helical AIE peptide probe and GO complex provided a highly specific sensing platform for the target charged collagen peptides. The robust analytical assay for charged collagen peptide fragments would signifcantly contribute to the development of diagnostic methods for collagen diseases.

Experimental section

Materials

Graphene oxide was purchased from Gezhi New Materials Co., Ltd. (Anqing, China). 1-(4-Carboxyphenyl)-1,2,2-triphenylethene (TPE) was obtained from Dibai Biotechnology Co., Ltd (Shanghai, China). All Fmoc-amino acids were purchased from GL Biochem Ltd. (Shanghai, China). HBTU (O-Benzotriazole-N,N,N',N'-tetramethyl-uronium-hexafluorophosphate) and HOBt (1-Hydroxybenzotriazole) was purchased from GL Biochem Ltd. (Shanghai, China). All the reagents obtained from commercial sources were of analytical grade and were used without further purification. Ultrapure water was used to prepare all the solutions.

Peptide synthesis

Peptide POG was provided by Chinese Peptide Company (Hangzhou, China). Peptides TPE-PRG (with amino acid sequence TPE-$G(PRGPOG)_5$), EOG (with amino acid sequence $G(EOG)_{10}$), POG (with amino acid sequence $G(POG)_{10}$), EOA (with amino acid sequence $G(EOG)_4EOA(EOG)_5$), G (with amino acid sequence FGGGGG), O (with amino acid sequence FOOOOO), H (with amino acid sequence FHHHHH), R (with amino acid sequence FRRRRR), K (with amino acid sequence FKKKKK), E (with amino acid sequence FEEEEE) and D (with amino acid sequence FDDDDD) were synthesized in-house by standard Fmoc solid phase synthesis method. Stepwise couplings of amino acids were carried out according to a double coupling method with Fmoc-amino acids (4 eq.), DIEA (N, N-Diisopropylethylamine， 6 eq.) and activator reagents (HBTU + HOBt 0.66 mmol/mL, 4 eq.). DMF (N, N-Dimethylformamide, 3 x 5 mL) and DCM (Dichloromethane, 3 x 5 mL) were employed to wash the reaction mixture after each step of coupling, and 20% piperidine was used to remove the Fmoc protection group. Test reagent (2% ethanal DMF, 2% chloranil DMF) was applied to determine the completion of each coupling reaction and Fmoc deprotetction. TPE-PRG was synthesized by conjugating TPE to the N-terminal of peptide $G(PRGPOG)_5$ by using TPE (12 eq.), DIEA (6 eq.) and activator reagent PyAOP [(3-Hydroxy-3H-1,2,3-triazolo[4,5-b]pyridinato-O)tri-1-pyrrolidinylphosphonium hexafluorophosphate, (12 eq.)] for 24 hrs. TFA (trifluoroacetic acid)/TIS (Triisopropylsilane)/H_2O (95:2.5:2.5) was used to treat the resin for 3 hrs in order to eliminate the tBu groups and to take the peptides off the resin. Cold Et_2O (Diethyl ether anhydrous) was used to precipitate the peptides, and the precipitates were resuspended in cold Et_2O, sonicated and centrifuged again. Crude products were purified using reverse phase HPLC (high pressure liquid chromatography) on a C18 column, and the purity of the peptides were confirmed by mass spectrometry. m/z calculated 3322.1 $[M]^+$ for TPE-PRG, found 3322.0 $[M]^+$; m/z calculated 3068.3 $[M]^+$ for EOG, found 3067.8 $[M]^+$; m/z calculated 3082.0 $[M]^+$ for EOA, found 3081.6 $[M]^+$; m/z calculated 450.5 $[M]^+$ for G, found 451.2 $[M]^+$; m/z calculated 730.8 $[M]^+$ for O, found 731.4 $[M]^+$; m/z calculated 946.2 $[M]^+$ for R, found 946.5 $[M]^+$; m/z calculated 806.1 $[M]^+$ for K, found 806.5 $[M]^+$; m/z calculated 741.0 $[M]^+$ for D, found 741.2 $[M]^+$; m/z calculated 851.0 $[M]^+$ for H, found 851.4 $[M]^+$; m/z calculated 810.8 $[M]^+$ for E, found 811.3 $[M]^+$.

Circular Dichroism Spectroscopy

Circular Dichroism (CD) spectra were recorded on an Aviv model 400 spectrophotometer (Applied Photophysics Ltd, UK) supplemented with a Peltier temperature controller. The samples of peptide TPE-PRG with a concentration of 1 mg/mL were prepared in 20 mM PBS buffer at pH 7.4. Cells with a path length of 1 mm were applied. Wavelength scans were measured from 200 to 260 nm with a 0.5 nm increment per step and a 0.5 s averaging time at 4 °C. Each measurement was repeated 3 times.

The thermal stability of the peptides was determined by monitoring the amplitude of the CD peak at 225 nm as a function of increasing temperature from 4 °C to 90 °C with an average heating rate of 0.5 °C/min and 2 min equilibration time. The peptides were heated at 90 °C for 20 min and then re-equilibrated at 4 °C for at least 24 hrs prior to the melting experiments. The first derivative of the thermal unfolding curve was computed and smoothed by the Savitzky-Golay method using a third-order polynomial. The melting temperature (T_m) was obtained as the extrema of the first derivative.

Fluorescence Assays

Fluorescence spectra were measured on a RF-5301PC fluorescence spectrometer (Shimadzu Instruments Ltd., Japan). Peptide TPE-PRG was dissolved in 20 mM PBS pH 7.4, and incubated at 90 °C for 20 min and at 4 °C for >24 hrs to drive the triple helix formation. Standard solutions of target peptide EOG were prepared by serial dilution. Fluorescence spectra were recorded after GO was added to the solution of peptide TPE-PRG (1 μM) at an excitation wavelength of 327 nm.

In the fluorescence assays of the target collagen peptide EOG, a “pre-mixing” strategy was used to allow sufficient interaction of probe peptide TPE-PRG and target peptide EOG. The probe peptide TPE-PRG (300 μM) was mixed with the target peptide EOG (100 μM) in 40 μL PBS buffer, and incubated at room temperature for

>15 min. The mixture was then diluted 300 times to obtain a final concentration of peptide TPE-PRG as 1 μM. The GO solution with a final concentration of 12 μg/mL was added into the mixture for fluorescence measurements. For the quantitative assay, different final concentrations of the target peptide EOG (20, 80, 100, 130, 150, 180, 200, 230, 250, 270, and 300 nM) were prepared in the mixture with the fluorescent probe peptide TPE-PRG, and the fluorescence spectra were recorded after the addition of 12 μg/mL GO. Standard solutions of peptides G, O, H, K, R, D, E and POG with a final concentration of 2 μM were prepared to investigate the interference of other peptides in the detection of the target peptide EOG. A high concentration of 1 mM of these nonspecific peptides were prepared and 6 μL of each peptide was added to the prepared TPE-PRG peptide solution or the TPE-PRG/EOG mixture, and then GO was added to start the fluorescence measurements. All the measurements were repeated for 3 times.

Results and discussion

Design of the triple helical AIE-peptide probe TPE-PRG

In addition to the neutral Pro-Hyp-Gly triplet, collagen is also rich in charged amino acids with Glu-Hyp-Gly as one of the most abundant charged triplets in Type I collagen. Therefore, peptide EOG (with amino acid sequence $G(EOG)_{10}$) is constructed to represent a typical charged amino acid-rich collagen fragment. Previous studies have suggested that collagen peptide $(PRGPOG)_5$ formed heterotrimer species with peptide $(EOG)_{10}$.[41] We have recently discovered that FITC-labeled triple helical peptide $C(POG)_9$ could recognize single stranded GPO-rich peptide.[40] We therefore hypothesize that triple-helical peptide $G(PRGPOG)_5$ may specifically bind with single-stranded target peptide $G(EOG)_{10}$.

In order to build an AIE-peptide probe based biosensor, a popular AIE-active fluorophore TPE was conjugated with peptide $G(PRGPOG)_5$ to create triple helical AIE-peptide probe TPE-PRG (with amino acid sequence TPE-$G(PRGPOG)_5$). It contains five charged amino acids per chain, leading to good water solubility. We hypothesize that peptide TPE-PRG in the monomer conformation in aqueous solution has weak fluorescence because of the free intramolecular torsional motion of nonplanar TPE, while the formation of triple helix dramatically enhance the fluorescence of the probe peptide due to the restriction of intramolecular rotation of TPE in the trimer state (Scheme 1).

Multiple Arg's are included in the AIE-peptide probe to enhance the interaction between the probe peptide and GO. The adsorption of the triple helical AIE-peptide probe TPE-PRG onto the surface of GO would efficiently quench the fluorescence of TPE moiety (Scheme 1). However, in the presence of monomeric target collagen peptide EOG, the binding of EOG with TPE-PRG would result in the desorption of the peptide probe from the surface of GO, therefore recovering the original fluorescence of the triple helical peptide probe TPE-PRG (Scheme 1).

Characterization of the probe peptide TPE-PRG

The formation of triple helix structure is considered as a key prerequisite for probe peptide TPE-PRG to possess strong fluorescence. Circular dichroism (CD) spectra of peptide TPE-PRG displayed a maximum absorption at 225 nm, demonstrating the formation of triple helix structure (Figure 1A). Thermal transition studies further showed that peptide TPE-PRG formed a stable triple helix with a melting temperature (T_m) of 65 °C at pH 7.4 in 20 mM PB buffer (Figure 1B). It indicated that the conjugation of fluorophore TPE enhanced the triple helix stability of peptide $(PRGPOG)_5$, which was likely due to the favorable hydrophobic interactions between the TPE groups.[41]

Fluorescence spectra of the probe peptide TPE-PRG were recorded at 25 °C and 90 °C (Figure 1C). The probe peptide TPE-PRG showed a weak fluorescence intensity at 90 °C, since it was in the monomer conformation, and the free intramolecular torsional motion of TPE would result in fast nonradiative relaxation and largely reduce the photoluminescence quantum yield.[42] Meanwhile, the probe peptide TPE-PRG showed much enhanced fluorescence intensity at 25 °C, since the formation of triple helix structure caused pronounced restriction of intramolecular rotation of TPE, leading to the closure of the nonradiative decay channel (Figure 1C). Furthermore, Figure 1D showed a visible emission color change of peptide TPE-PRG at 25 °C and 90 °C at UV light. The peptide displayed a cyan color in the trimer state at 25 °C, while it became colorless in the monomer state at 90 °C (Figure 1D). These results confirmed our hypothesis that triple helical AIE-peptide probe TPE-PRG possessed strong fluorescence.

Characterization of GO

The purchased GO was characterized by XRD, Raman, FTIR and TEM techniques (Figure S1). The XRD pattern of GO showed an intense peak at $2\theta = 10°$, which corresponded to the characteristic interlayer space of GO due to the presence of oxygen-containing functional groups on the GO sheets (Figure S1A). The Raman spectrum of GO indicated a distinct peak assigned to the vibration of SP^2-bonded carbon atoms at 1597 cm^{-1} (G band) and another strong peak corresponding to the vibration of carbon atoms with dangling bonds at 1339 cm^{-1} (D band), which were consistent with previous reports (Figure S1B).[40, 43-45] The FTIR spectrum of GO showed characteristic peaks at 3412 cm^{-1} (O-H bond), 1729 cm^{-1} (C=O bond), 1623 cm^{-1} (the vibrations of unoxidized graphitic skeletal domains and the adsorbed water molecules), 1216 cm^{-1} (C-OH bond) and 1053 cm^{-1} (C-O bond) (Figure S1C).[40, 43, 45] The TEM image showed a typical layered structure of GO, that has been widely observed (Figure S1D).[40, 44-46] The XRD, Raman, FTIR and TEM results demonstrated the successful fabrication of GO.

The fluorescence quenching of TPE-PRG by GO

The fluorescence emission spectra were recorded for the triple helical probe peptide TPE-PRG in the presence of various concentrations of GO (0-13.33 μg/mL) (Figure 2). The peptide TPE-PRG alone showed strong fluorescence at 472 nm. With the addition of GO, the fluorescence intensity of TPE-PRG became gradually decreased. When the concentration of GO reached 12 μg/mL, the fluorescence of TPE-PRG was almost completely quenched (Figure 2). The quenching efficiency of the GO was estimated as 91%, and the high quenching efficiency would result in improved sensitivity and a broad dynamic range for target detection.

View Article Online
DOI: 10.1039/D0TB00476F

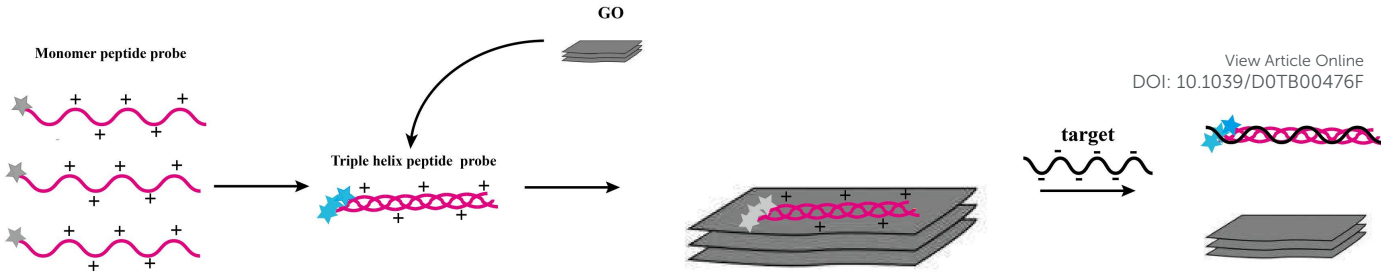

Scheme 1. Schematic Illustration of the concept of using a triple helical AIE-peptide probe and GO platform to detect target collagen sequence.

Monitoring the interaction of probe peptide TPE-PRG and charged target collagen peptide EOG

The fluorescence response of the probe peptide TPE-PRG with various concentrations of target peptide EOG was investigated in the presence of GO in 20 mM PBS buffer, pH 7.4 (Figure 3). The TPE-PRG/GO platform showed a relatively low fluorescence intensity in the absence of peptide EOG (Figure 3A). Upon the addition of charged target peptide EOG, the fluorescence intensity of the TPE-PRG/GO platform was markedly enhanced. As the concentration of peptide EOG increased, the fluorescence intensity at 472 nm gradually increased, which reached a plateau when the concentration of EOG became 3.0 μM or higher (Figure 3B). The enhancement of the fluorescence intensity after the addition of EOG suggested that the binding of target peptide EOG with probe peptide TPE-PRG led to its desorption from the surface of GO.

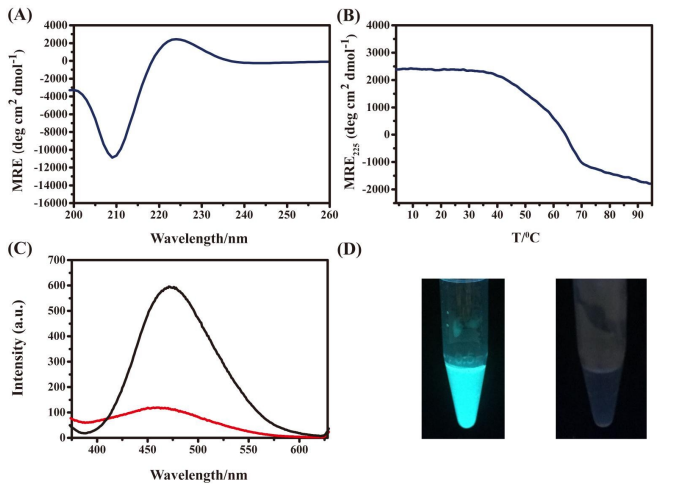

Figure 1. Characterization of the probe peptide TPE-PRG. (A) CD wavelength scans and (B) thermal transitions of the peptide. Melting transitions were monitored by CD spectroscopy at 225 nm. (C) Fluorescent profiles of the probe peptide incubated at 25 °C (black) and heated to 90 °C for 20 min (red). The emission spectra were recorded at an excitation wavelength of 327 nm. (D) Visual changes of the probe peptide incubated at 25 °C (left) and heated to 90 °C for 20 min (right) under a UV lamp.

Notably, a linear relationship was observed between the concentration of target peptide EOG and the changes of fluorescence intensity at 472 nm (R^2=0.99) (Figure 4). This TPE-PRG/GO sensing platform showed a broad linear range from 20 to 300 nM (Figure 4). Furthermore, it allowed the accurate determination of peptide EOG at a concentration as low as 17 nM, which was comparable to previous reports of the detection of a neutral collagen peptide with rich imno acids.[40]

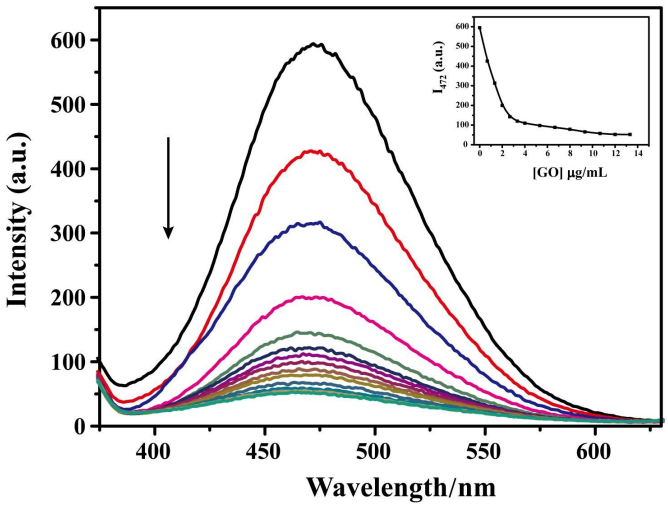

Figure 2. The fluorescence quenching of the triple helical probe peptide TPE-PRG by various concentrations of GO. The fluorescence emission spectra were recorded for the probe peptide TPE-PRG in the presence of various concentrations of GO (0, 0.67, 1.33, 2.0, 2.67, 3.33, 4.0, 5.33, 6.67, 8.0, 9.33, 10.67, 12, 13.33 μg/mL). Inset: the fluorescence intensity monitored at 472 nm as a function of GO concentration.

The fluorescence restoration capability of target peptide EOG toward the probe peptide TPE-PRG was further evaluated in the presence of GO under different pHs (Figure S2). The TPE-PRG/GO complex in the absence of target peptide EOG showed consistently low florescence intensity from pH 6.0 to 9.0, suggesting the high quenching efficiency of GO toward triple helical probe peptide TPE-PRG in this pH range. In the presence of target peptide EOG, the TPE-PRG/GO complex displayed similarly enhanced fluorescence from pH 6.0 to 9.0, indicating that the target peptide could effectively bind with the probe peptide and release it from the GO surface around physiological pH conditions (Figure S2).

Binding stoichiometry

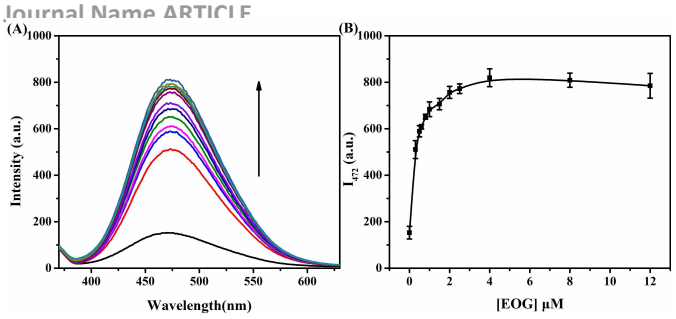

Figure 3. The interaction between probe peptide TPE-PRG and target collagen peptide EOG. The fluorescence emission spectra of the TPE-PRG/GO complex were recorded before and after the addition of increasing concentrations of peptide EOG (A). The fluorescence intensity monitored at 472 nm (I_{472}) as a function of the concentration of peptide EOG (B).

A Job's analysis was carried out to determine the binding stoichiometry of the probe peptide TPE-PRG and EOG by keeping the sum of the concentrations of both peptides at 1 μM. The fluorescence emission intensity change at 472 nm versus the mole fraction of the target peptide EOG was measured. The maximum emission intensity change was observed at a mole fraction of about 0.25 (Figure S3). This suggested that peptides TPE-PRG and EOG probably formed a 3 TPE-PRG : 1 EOG complex.

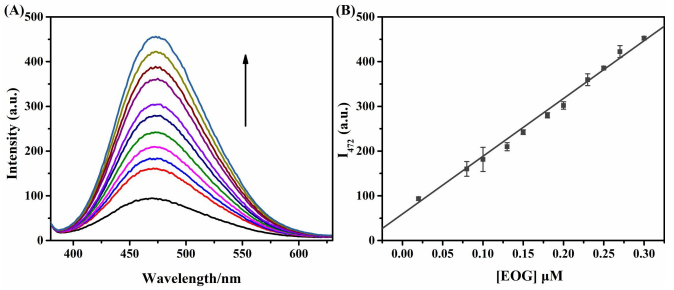

Figure 4. The linear fluorescence restoration of the TPE-PRG/GO platform by the target peptide EOG. The fluorescence emission spectra were recorded for the TPE-PRG/GO platform in the presence of various concentrations of peptide EOG (0, 20, 80, 100, 130, 150, 180, 200, 230, 250, 270, 300 nM) (A). The changes of the fluorescence intensity monitored at 472 nm (I_{472}) as a function of the concentration of the target peptide EOG (B).

Specificity of the TPE-PRG/GO based fluorescence assay

The specificity of the fluorescence assay using the TPE-PRG/GO platform was examined (Figure 5). The fluorescence intensities were measured for the TPE-PRG/GO complex in the presence of peptides G (with amino acid sequence FGGGGG), O (with amino acid sequence FOOOOO), H (with amino acid sequence FHHHHH), R (with amino acid sequence FRRRRR), K (with amino acid sequence FKKKKK), E (with amino acid sequence FEEEEE), D (with amino acid sequence FDDDDD) and POG (with amino acid sequence $G(POG)_{10}$) (red). Compared with the target peptide EOG, all these peptides showed much less florescence recovery, indicating that the TPE-PRG probe was highly specific for the target collagen sequence EOG. Furthermore, the fluorescence restoration of the probe peptide TPE-PRG by the target peptide EOG was evaluated in the absence

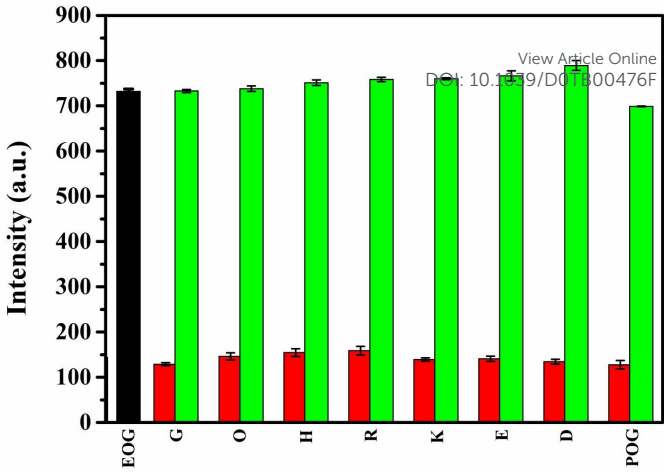

Figure 5. The fluorescence restoration of the probe peptide TPE-PRG by other peptides. The fluorescence intensities at 472 nm were recorded for the probe TPE-PRG bound with the target peptide EOG (black). The fluorescence intensities at 472 nm were measured for the probe TPE-PRG in the presence of other peptides alone (red) and together with EOG (green).

and presence of these peptides (green). Compared with the target peptide EOG alone, the peptide EOG together with these peptides displayed similar fluorescence recovery, suggesting little interference of these peptides in the detection of EOG (Figure 5). These results demonstrated that the TPE-PRG/GO platform provided a sensitive and selective probe for the detection of target collagen peptide EOG without the interferences of other peptides.

Distinguishing target peptide from its mutant type using the TPE-PRG/GO platform

Single amino acid mutation in Type I collagen is the main cause of a variety of connective tissue disorders including Osteogenesis Imperfecta and Ehlers-Danlos syndrome.[47, 48] Therefore, the development of analytical assays that can distinguish natural collagen sequences from its mutant type is essential for the diagnosis and treatment of collagen diseases. The fluorescence restoration of the probe peptide TPE-PRG by peptide EOA (with amino acid sequence $G(EOG)_4EOA(EOG)_5$), which contained a single amino acid mutation from its parent collagen peptide EOG, was examined. Fluorescence emission profiles were recorded for the probe peptide TPE-PRG alone (black), the probe peptide complexed with EOG (red), and the probe peptide complexed with mutant peptide EOA (blue) (Figure 6). In contrast with target peptide EOG, the mutant peptide EOA barely enhanced the fluorescence intensity of the probe peptide TPE-PRG, indicating that peptide EOA could not interact with peptide TPE-PRG. Recent studies revealed that the constructed FITC-GPO/GO plaform could interact with peptides rich in GPO triplets with or without interruptions.[40] In contrast, this TPE-PRG/GO biosensor was very specific for peptide EOG, and even a single mutation of the target peptide would completely eliminate the recognition. To conclude, the TPE-PRG/GO complex provided a robust approach that can distinguish the target collagen peptide EOG from its single amino acid mutant type.

Conclusion

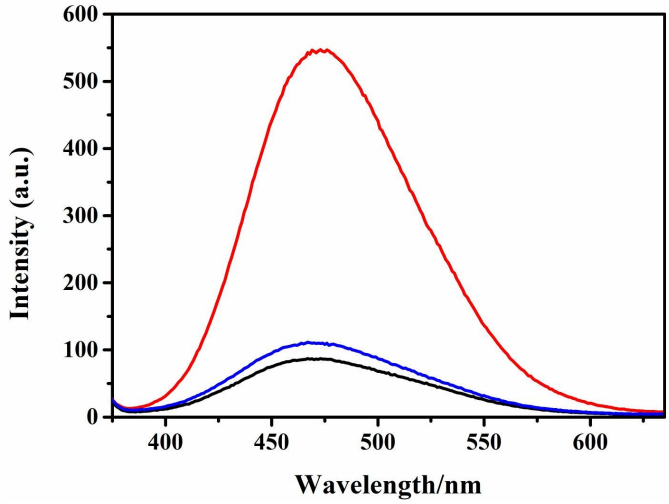

Figure 6. The fluorescence restoration of the probe peptide TPE-PRG by target peptide with a single amino acid mutation. Fluorescence emission profiles were recorded for the probe peptide TPE-PRG alone (black), the probe peptide complexed with EOG (red), and the probe peptide complexed with peptide EOA containing a single amino acid mutation (blue).

Aggregation-induced emission (AIE) probes have attracted increasing attention as versatile "turn-on" sensing platforms for biomolecules such as DNAs and proteins.[12] However, the potential interferential interaction of the AIE probes with other molecules may limit the selectivity of the assay.[24] Recent studies suggested that the construction of AIE biosensors with the aid of graphene oxide (GO) may be a promising strategy for developing biological assays with improved selectivity.[25] Collagen is a critical biomarker involved in a number of severe diseases, and its amino acid sequence pattern is characterized by the repetitive GPO triplet as well as a high content of charged amino acids. We have recently developed a GO-based biosensor for the detection of unfolded collagen peptides with neutral GPO triplets.[40]

We herein for the first time report the development of a GO-aided AIE "turn-on" biosensor for the highly specific detection of a typical charged collagen peptide. We have designed and synthesized a novel triple helical AIE probe peptide TPE-PRG with good water solubility. CD and fluorescent characterization indicates that the probe peptide TPE-PRG displays strong fluorescence in the trimer state due to the restriction of intramolecular rotation of TPE. The positively charged triple helical probe peptide TPE-PRG could be adsorbed onto the surface of GO, leading to efficient quenching of the fluorescence of TPE moiety. Meanwhile, the competitive binding of the probe peptide TPE-PRG with the negatively charged target collagen peptide EOG to form a 3:1 complex disrupts the interaction between TPE-PRG and GO, resulting in the restoration of the fluorescence of the probe.

The probe peptide TPE-PRG/GO platform has been demonstrated as highly selective to the charged collagen peptide EOG, showing little interference from other peptides. Furthermore, it could perfectly distinguish the target peptide EOG from its single amino acid mutant type. The TPE-PRG/GO biosensor provides a robust strategy for the detection of charged collagen peptides, which remarkably enhances our capability to understand the degradtion process of collagen, showing promising applications in molecular diagnostics of collagen diseases.

View Article Online
DOI: 10.1039/D0TB00476F

Conflicts of interest

The authors declare no competing conflict of interests.

Associated Content

Supporting Information

The Supporting Information is available free of charge on the ACS Publications website.

Acknowledgements

This work was supported by grants from the National Natural Science Foundation of China (Grant No. 21775059) and the Fundamental Research Funds for the Central Universities (Grant No. lzujbky-2018-78).

References

1 X. Luo, J.J. Davis, *Chem Soc Rev.* 2013, **42**, 5944-5962.
2 C.A. Borrebaeck, *Nat Rev Cancer.* 2017, **17**, 199-204.
3 M.W. Peczuh, A.D. Hamilton, *Chem Rev.* 2000, **100**, 2479-2494.
4 F. Ma, Y. Li, B. Tang, C.Y. Zhang, *Acc Chem Res.* 2016, **49**, 1722-1730.
5 J. Wu, W. Liu, J. Ge, H. Zhang, P. Wang, *Chem Soc Rev.* 2011, **40**, 3483-3495.
6 M. Sauer, *Angew Chem Int Ed Engl.* 2003, **42**, 1790-1793.
7 B.T. Bajar, E.S. Wang, S. Zhang, M.Z. Lin, J. Chu, *Sensors (Basel).* 2016, **16**, 1488-1512.
8 D. Ding, K. Li, B. Liu, B.Z. Tang, *Acc Chem Res.* 2013, **46**, 2441-2453.
9 Y. Huang, J. Xing, Q. Gong, L.C. Chen, G. Liu, C. Yao, Z. Wang, H.L. Zhang, Z. Chen, Q. Zhang, *Nat Commun.* 2019, **10**, 169.
10 N. Zhao, J.W. Lam, H.H. Sung, H.M. Su, I.D. Williams, K.S. Wong, B.Z. Tang, *Chemistry.* 2014, **20**, 133-138.
11 J. Luo, Z. Xie, J.W. Lam, L. Cheng, H. Chen, C. Qiu, H.S. Kwok, X. Zhan, Y. Liu, D. Zhu, B.Z. Tang, *Chemical communications.* 2001, 1740-1741.
12 J. Mei, N.L. Leung, R.T. Kwok, J.W. Lam, B.Z. Tang, *Chem Rev.* 2015, **115**, 11718-11940.
13 Y. Hong, J.W. Lam, B.Z. Tang, *Chem Soc Rev.* 2011, **40**, 5361-5388.
14 X. Ni, X. Zhang, X. Duan, H.L. Zheng, X.S. Xue, D. Ding, *Nano Lett.* 2019, **19**, 318-330.
15 C. Chen, H. Ou, R. Liu, D. Ding, *Adv Mater.* 2020, **32**, 1806331-1806336.
16 C. Chen, X. Ni, H.W. Tian, Q. Liu, D.S. Guo, D. Ding, *Angew Chem Int Ed Engl.* 2020, DOI: 10.1002/anie.201916430.
17 C. Chen, X. Ni, S. Jia, Y. Liang, X. Wu, D. Kong, D. Ding, *Adv Mater.* 2019, **31**, DOI:10.1002/adma.201904914.
18 Y. Hong, J.W. Lam, B.Z. Tang, *Chemical communications.* 2009, 4332-4353.
19 S. Xie, A.Y.H. Wong, S. Chen, B.Z. Tang, *Chemistry.* 2019, **25**, 5824-5847.
20 Y. Hong, M. Haussler, J.W. Lam, Z. Li, K.K. Sin, Y. Dong, H. Tong, J. Liu, A. Qin, R. Renneberg, B.Z. Tang, *Chemistry.* 2008, **14**, 6428-6437.
21 M. Wang, D. Zhang, G. Zhang, Y. Tang, S. Wang, D. Zhu, *Analytical chemistry.* 2008, **80**, 6443-6448.
22 H. Tong, Y. Hong, Y. Dong, M. Haussler, J.W. Lam, Z. Li, Z. Guo, Z. Guo, B.Z. Tang, *Chemical communications.* 2006, 3705-3707.
23 J. Mei, Y. Hong, J.W. Lam, A. Qin, Y. Tang, B.Z. Tang, *Adv Mater.* 2014, **26**, 5429-5479.
24 H. Tong, Y. Hong, Y. Dong, M. Haussler, Z. Li, J.W. Lam, Y.

View Article Online
DOI: 10.1039/D0TB00476F

Dong, H.H. Sung, I.D. Williams, B.Z. Tang, *The journal of physical chemistry. B.* 2007, **111**, 11817-11823.
25 X. Xu, J. Huang, J. Li, J. Yan, J. Qin, Z. Li, *Chemical communications.* 2011, **47**, 12385-12387.
26 X. Xu, J. Li, Q. Li, J. Huang, Y. Dong, Y. Hong, J. Yan, J. Qin, Z. Li, B.Z. Tang, *Chemistry.* 2012, **18**, 7278-7286.
27 A. Tyagi, K.L. Chu, I.H. Abidi, A.A. Cagang, Q. Zhang, N.L.C. Leung, E. Zhao, B.Z. Tang, Z. Luo, *Acta Biomater.* 2017, **50**, 334-343.
28 H. Wang, K. Ma, B. Xu, W. Tian, *Small.* 2016, **12**, 6613-6622.
29 X. Li, K. Ma, S. Zhu, S. Yao, Z. Liu, B. Xu, B. Yang, W. Tian, *Analytical chemistry.* 2014, **86**, 298-303.
30 G.P. Riley, R.L. Harrall, P.G. Watson, T.E. Cawston, B.L. Hazleman, *Eye (Lond).* 1995, **9 (Pt 6)**, 703-718.
31 M.D. Sternlicht, Z. Werb, *Annu Rev Cell Dev Biol.* 2001, **17**, 463-516.
32 G.B. Fields, *J Biol Chem.* 2013, **288**, 8785-8793.
33 M.E.G. C. M. Kielty, *Eds. Wiley Liss: New York.* 2002, 159-222.
34 P. Caravan, B. Das, S. Dumas, F.H. Epstein, P.A. Helm, V. Jacques, S. Koerner, A. Kolodziej, L. Shen, W.C. Sun, Z. Zhang, *Angew Chem Int Ed Engl.* 2007, **46**, 8171-8173.
35 J. Mueller, F.C. Gaertner, B. Blechert, K.P. Janssen, M. Essler, *Mol Cancer Res.* 2009, **7**, 1078-1085.
36 F. Pernasetti, J. Nickel, D. Clark, P.A. Baeuerle, D. Van Epps, B. Freimark, *Int J Oncol.* 2006, **29**, 1371-1379.
37 J. Xu, D. Rodriguez, J.J. Kim, P.C. Brooks, *Hybridoma.* 2000, **19**, 375-385.
38 G.R. Srinivas, C.O. Chichester, H.J. Barrach, V. Pillai, A.L. Matoney, *Immunol Invest.* 1994, **23**, 85-98.
39 C. Chichester, H.J. Barrach, A. Chichester, A. Matoney, G.R. Srinivas, *J Immunol Methods.* 1991, **140**, 259-267.
40 X.X. Sun, J. Fan, Y.P. Zhang, H.L. Chen, Y.Q. Zhao, J.X. Xiao, *Biosensors & Bioelectronics.* 2016, **79**, 15-21.
41 L.E. O'Leary, J.A. Fallas, J.D. Hartgerink, *J Am Chem Soc.* 2011, **133**, 5432-5443.
42 M. Dommett, M. Rivera, R. Crespo-Otero, *The journal of physical chemistry letters.* 2017, **8**, 6148-6153.
43 C.H. Lu, J. Li, X.L. Zhang, A.X. Zheng, H.H. Yang, X. Chen, G.N. Chen, *Analytical chemistry.* 2011, **83**, 7276-7282.
44 P.M. Sabale, J.T. George, S.G. Srivatsan, *Nanoscale.* 2014, **6**, 10460-10469.
45 H. Liu, Y. Wang, A. Shen, X. Zhou, J. Hu, *Talanta.* 2012, **93**, 330-335.
46 S. Nandi, P. Routh, R.K. Layek, A.K. Nandi, *Biomacromolecules.* 2012, **13**, 3181-3188.
47 J.C. Marini, A. Forlino, W.A. Cabral, A.M. Barnes, J.D. San Antonio, S. Milgrom, J.C. Hyland, J. Korkko, D.J. Prockop, A. De Paepe, P. Coucke, S. Symoens, F.H. Glorieux, P.J. Roughley, A.M. Lund, K. Kuurila-Svahn, H. Hartikka, D.H. Cohn, D. Krakow, M. Mottes, U. Schwarze, D. Chen, K. Yang, C. Kuslich, J. Troendle, R. Dalgleish, P.H. Byers, *Hum Mutat.* 2007, **28**, 209-221.
48 R. Dalgleish, *Nucleic Acids Res.* 1997, **25**, 181-187.

Table of content

View Article Online
DOI: 10.1039/D0TB00476F

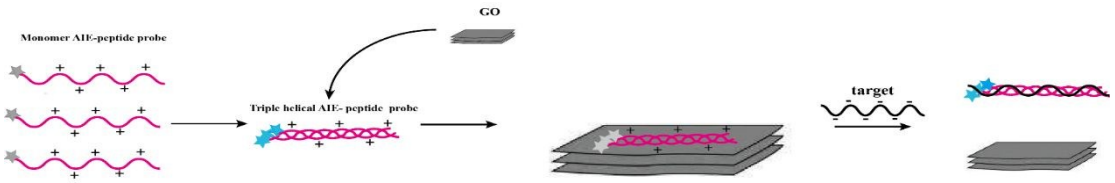

A graphene oxide-aided triple helical aggregation-induced emission biosensor provides a highly specific sensing platform for charged collagen peptides